

## Large-scale structure of RecA protein from *Deinococcus radiodurance* and its complexes in solution

This article has been downloaded from IOPscience. Please scroll down to see the full text article.

2008 J. Phys.: Condens. Matter 20 104215

(<http://iopscience.iop.org/0953-8984/20/10/104215>)

View [the table of contents for this issue](#), or go to the [journal homepage](#) for more

Download details:

IP Address: 129.252.86.83

The article was downloaded on 29/05/2010 at 10:42

Please note that [terms and conditions apply](#).

# Large-scale structure of RecA protein from *Deinococcus radiodurance* and its complexes in solution

D V Karel'ov<sup>1</sup>, D V Lebedev<sup>1</sup>, A V Suslov<sup>1</sup>, V I Shalguev<sup>1</sup>,  
A I Kuklin<sup>2</sup>, A Kh Islamov<sup>2</sup>, H Lauter<sup>3</sup>, V A Lanzov<sup>1</sup> and  
V V Isaev-Ivanov<sup>1</sup>

<sup>1</sup> Petersburg Nuclear Physics Institute, Gatchina, Russian Federation

<sup>2</sup> Joint Institute for Nuclear Research, Dubna, Russian Federation

<sup>3</sup> Institute Max von Laue Paul Langevin, Grenoble, France

Received 16 July 2007, in final form 31 October 2007

Published 19 February 2008

Online at [stacks.iop.org/JPhysCM/20/104215](http://stacks.iop.org/JPhysCM/20/104215)

## Abstract

Different conformational states of the filaments formed by RecA protein from a radiation resistant strain *Deinococcus radiodurance* (RecA<sub>Dr</sub>) in solution were investigated using small angle neutron scattering. Scattering by the protein self-polymer was consistent with a long helix model, with the pitch of the helix being lower than that in the crystal structure. Compared to those of RecA proteins from *Escherichia coli* and *Pseudomonas aeruginosa*, helical filaments of RecA from *D. radiodurance* exhibited a lower helical pitch and lower stability at low Mg<sup>2+</sup> concentrations or under conditions of elevated ionic strength in the absence of ATP (adenosine triphosphate). Formation of an active filament upon binding of ATPγS and either single- or double-stranded DNA brought about a significant increase in the helix pitch and a moderate decrease in the cross-sectional gyration radius, but resulted in little change in the number of monomers per helix turn. The helix pitch value of the RecA<sub>Dr</sub> presynaptic complex was conservative and close to that found for other RecA proteins and their analogs.

## 1. Introduction

*Deinococcus radiodurance* is the most radiation resistant species currently known (LD<sub>37</sub> = 5.5 kGy compared to 0.17 kGy for *E. coli*). These bacteria exhibit unusual features in genome organization, regulation of post-radiation DNA degradation, homologous recombination and replication [1], but the exact mechanism of the extreme radiation resistance remains unclear. Homologous recombination protein RecA plays a key role in DNA repair following radiation damage in bacteria. A single mutation in *recA* gene in *D. radiodurance* with one amino acid substitution (RecA<sub>Dr</sub>670) abolishes radiation resistant property of this organism [1].

Some RecA<sub>Dr</sub> biochemical characteristics differ from those described for RecA from *Escherichia coli* (RecA<sub>Ec</sub>) [2]. RecA<sub>Dr</sub> possesses an unusually high affinity for double-stranded DNA (dsDNA). While a general mechanism of homologous recombination requires the formation of presynaptic complex between RecA and single-stranded DNA (ssDNA) before the strand exchange with homologous dsDNA,

the RecA<sub>Dr</sub> protein exhibits preferential formation of the presynaptic complex on dsDNA [2, 3].

The x-ray crystallographic structure of RecA from *D. radiodurance* [4] exhibits usual for these proteins helical symmetry but with a lower helical pitch than seen in RecA protein from *E. coli* [5, 6]. Similar to other RecA proteins, it has a 3-domain structure. The N-terminal domain is substantially larger than in *E. coli* RecA. Up to date a substantial amount of observation has been accumulated that show that the filament of RecA protein and its functional analogs is a highly flexible structure. The geometry of the filaments in solution depends on substrate and co-factor binding as well as the solvent properties and generally differs from that derived from the crystal structure [7–11]. In a number of works two types of filament conformations have been observed, an 'open' conformation assumed upon binding of DNA and ATP in the presence of Mg<sup>2+</sup>, and 'closed' conformation, which is formed upon polymerization of the protein alone or in a complex with DNA in the absence of ATP [11]. An open conformation, thought to correspond to the

active form of the enzyme, has significantly higher helical pitch and lower cross-sectional gyration radius than the 'closed' form. The pitch of the presynaptic complex appear to be conserved ( $\sim 85\text{--}95$  Å), matching the pitch of the extended form of dsDNA [12]. Unwinding of dsDNA from B-form to the extended form is thought to be a part of the enzyme function and the respective 1.5-fold elongation of RecA–DNA nucleoprotein complex has been observed experimentally [13].

In this work we used SANS to determine the geometry of the filaments formed by RecA protein from *D. radiodurance* in solution in different functional states, particularly of the inactive protein polymer and the presynaptic complexes of the enzyme with ssDNA and dsDNA.

## 2. Experimental procedures

Wild-type *D. radiodurance* recA gene was cloned into pET-21b over-expression vector under regulation by phage T7 promoter and transformed into *E. coli* strain BL21(DE3). The protein was induced with 1 mM isopropyl- $\beta$ -D-thiogalactopyranoside for 2 h. All subsequent steps were performed at 4 °C. The centrifuged cells were resuspended in buffer A (250 mM Tris-HCl (pH 7.5), 25% (w/v) sucrose) containing lysozyme (final concentration, 1 mg ml<sup>-1</sup>) and stirred for 2 h. After addition EDTA (final concentration, 10 mM) to the cell lysate the cell suspension was treated with ultrasound 40 times for 10 s and centrifuged for 30 min at 15 000 *g*. Polymin P (final concentration, 0.5% v/v) was added to the supernatant, stirring for 30 min. The solution was centrifuged for 15 min at 10 000 *g*. The precipitate was resuspended in buffer R (20 mM Tris-HCl (pH 7.5), 10% (w/v) glycerol, 1 mM DTT, and 0.1 mM EDTA) containing 50 mM ammonium sulfate. The suspension was stirred for 30 min and centrifuged for 15 min at 10 000 *g*. To elute RecA protein the precipitate was resuspended in buffer R containing 200 mM ammonium sulfate. The suspension was stirred for 30 min and centrifuged for 15 min at 10 000 *g*. Ammonium sulfate (0.4 g ml<sup>-1</sup>) was added to the supernatant, it was stirred for 4–12 h and then centrifuged for 15 min at 10 000 *g* to collect precipitated RecA protein. The precipitate was dissolved in buffer P (20 mM potassium phosphate, pH 6.8) containing 200 mM NaCl and dialyzed overnight against the same buffer. After dialysis the solution was applied on a chromatographic column with phosphocellulose equilibrated with buffer P containing 200 mM NaCl. The flow-through fraction was collected and dialyzed against buffer R containing 50 mM KCl. Further the solution was applied on a chromatographic column with DEAE-Sepharose equilibrated with buffer R containing 50 mM KCl. The flow-through fractions were analyzed by SDS-PAGE and fractions containing RecA protein was brought together. Ammonium sulfate (0.4 g ml<sup>-1</sup>) was added to the supernatant, it was stirred for 4–12 h and then centrifuged for 15 min at 10 000 *g*. The precipitate was dissolved in buffer R and dialyzed against buffer R containing 100 mM KCl and 50% glycerol. The last dialysis was performed against D<sub>2</sub>O buffer containing 50% glycerol by volume. Protein was stored at 60–120 mg ml<sup>-1</sup> concentration at –30 °C. Protein concentrations were determined by

optical absorption at 280 nm using an extinction coefficient  $\epsilon_{280} = 10\,240$  M<sup>-1</sup> cm<sup>-1</sup>. Single-stranded DNA from phage M13mp19 was purified as described in [14], and its concentration determined by optical absorption at 260 nm, using the extinction coefficient of  $6.5 \times 10^3$  M<sup>-1</sup> cm<sup>-1</sup>. ATP $\gamma$ S and ADP were purchased from Sigma Chemical, Tris and MgCl<sub>2</sub> from Akros.

SANS data were acquired on YuMO spectrometer, Frank Laboratory of Nuclear Physics, Joint Institute for Nuclear Research in Dubna, Russia, and on D-11 spectrometer (ILL, Grenoble, France). On YuMO the standard time-of-flight acquisition method was used [15] with the collimated beam diameter of 14 mm and the range of neutron wavelengths from 0.7 to 6 Å. The raw data were processed and normalized as described in [15] to obtain the absolute values for the scattering intensity. Two detectors were used for simultaneous acquisition in the range of  $Q$  from 0.006 to 0.2 Å<sup>-1</sup>. Measurements on D-11 spectrometer were performed at two detector positions, 2 and 8 m, with the neutron wavelength at 6 Å. Samples were placed in 2 mm Helma cuvettes and were maintained at 15 °C in a temperature-stabilized box during measurements.

The measurements were performed at 15 °C in >99.8% D<sub>2</sub>O 20 mM tris-HCl buffer (pH 7.5) containing 10 mM Mg acetate and 3–5% glycerol. Blank sample of the buffer containing the same amount of glycerol was used as reference. ATP $\gamma$ S and/or M13 ssDNA (6 nucleotides per RecA monomer) or dsDNA (4 bp per RecA monomer) were added at the day of the experiment with subsequent incubation for 15 min at 37 °C. RecA concentration was 4–6 mg ml<sup>-1</sup>. The acquisition time for each curve was 20–60 min. The total duration of the experiment was no longer than 12 h.

Data were fitted to scattering by a long helical object in the approximation of the first diffraction maximum using the equations derived in [10, 16], as described in [10]

$$I(Q) = I_c(0) \left( J_0^2 \left( Q \sqrt{R_c^2 - 3r^2/5} \right) \Phi^2(Q) + 2\Psi^2(Q) \right), \quad (1)$$

where

$$\Psi(Q) = \begin{cases} J_1 \left( Q \sqrt{R_c^2 - 3r^2/5} \sqrt{1 - \left( \frac{2\pi}{hQ} \right)^2} \right) \Phi(Q), & Q \geq 2\pi/h \\ 0, & Q < 2\pi/h \end{cases} \quad (2)$$

$R_c$ —cross-sectional radius of gyration of the filament,  $h$ —helical pitch,  $r$  is the approximate radius of the monomer,  $J_0$  and  $J_1$  are Bessel functions,  $\Phi(Q) = 3(\sin(Qr) - Qr \cos(Qr))/(Qr)^3$  is the normalized form factor of a sphere. Zero-angle scattering approximation  $I_c(0) = [I(Q)Q]_{Q \rightarrow 0}$  was also performed from the fit, except in the case of scattering by non-filamentous structures. In the latter case Guinier approximation was used to calculate  $I(0)$  and the molecular weight of the scatterer

$$M_r = \frac{I(0)}{C N_A v^2 \Delta \rho^2}, \quad (3)$$

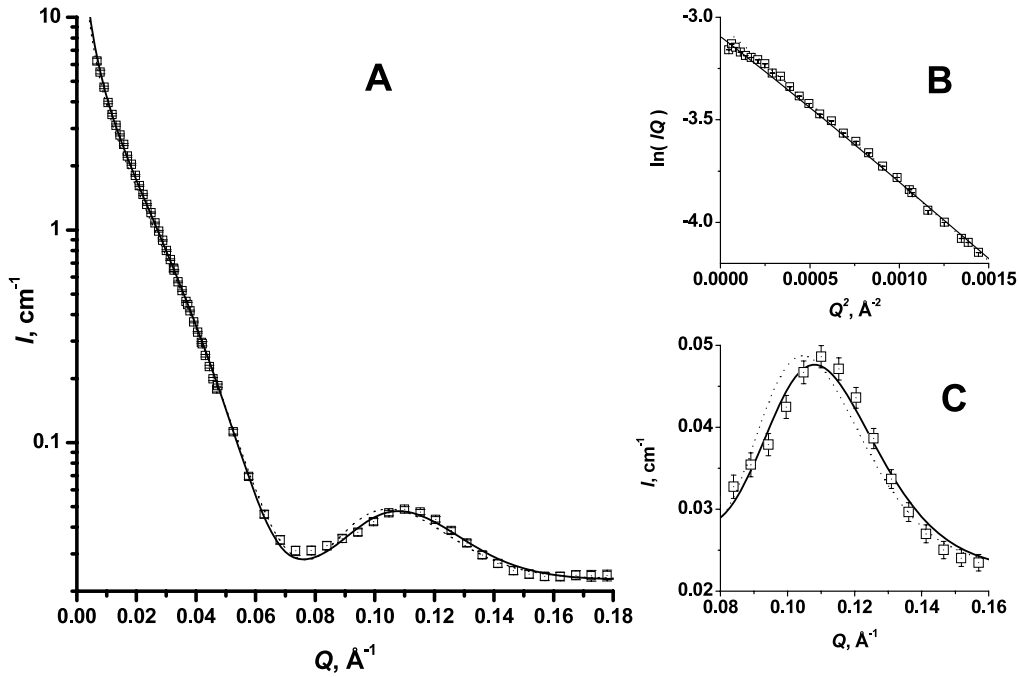


**Figure 1.** (A) Scattering curve of self-polymer of RecA<sub>D<sub>r</sub></sub> in D<sub>2</sub>O tris-HCl buffer (pH 7.5) containing 10 mM Mg<sup>2+</sup> (panel (A)). Data acquired on D11 spectrometer and fitted to the model for long helical filament [10], with helical pitch 63 Å, cross-sectional radius of gyration 39.8 Å and  $I_c(0)$  of 0.045 cm<sup>-1</sup> Å<sup>-1</sup>,  $\chi^2 = 1.2$  (solid line). Dashed line shows the same fit with the pitch fixed at 67 Å ( $\chi^2 = 3.1$ , dashed line). (B) Guinier region of the spectrum; solid line shows the model fit, dashed line—the linear fit (slope =  $-767 \text{ \AA}^2$ ). (C) Region of the scattering curve shown in panel (A) showing the subsidiary maximum.

where  $C$  is the weight concentration of the protein;  $N_A$  is Avogadro's number;  $v$  is the excluded volume per unit weight of the protein (approximately  $1.25 \text{ \AA}^3 \text{ Da}^{-1}$ ) and  $\Delta\rho = \rho - \rho_s$ —difference between the scattering densities of the protein and solvent [17].

Molecular weight per unit length of the filament,  $\mu$ , was calculated as

$$\mu = \frac{I_c(0)}{\pi C N_A v^2 \Delta\rho^2}. \quad (4)$$

Scattering density for D<sub>2</sub>O buffer containing 4.2% glycerol was taken as  $6.1 \times 10^{10} \text{ cm}^{-2}$  and the protein scattering density was taken as  $2.95 \times 10^{10} \text{ cm}^{-2}$  [17]. The number of monomers per helix turn and per oligomer was determined by equations (3) and (4) using the molecular weight of the monomer of 38.01 kDa.

### 3. Results and discussion

SANS spectrum of the RecA protein self-polymer from *D. radiodurans* formed in the presence of Mg<sup>2+</sup> is shown in figure 1. At low angles the curve followed the scattering law by rod-like particles and exhibited subsidiary maximum in the region of  $Q \sim 0.1 \text{ \AA}^{-1}$  that is a characteristic for scattering by the helical filaments of other RecA proteins [7]. The data could be fitted to a model curve [10] describing scattering for long helical filament with helical pitch of 63 Å and the cross-sectional radius of gyration of 39.8 Å. Cross-sectional radius of gyration was also estimated directly from the Guinier approximation for rod-like particles at low angles (figure 1(B)).

The value of 39.2 Å was slightly lower than that obtained from the model fit. The small difference between the two estimates could be related to slight deviation from linearity in the Guinier plot in the very small scattering angles (figure 1(B)), possibly caused by finite filament length or interference of the neighbouring filaments. The estimate yielded by the first approach should be considered more reliable as it is based on the entire scattering curve rather than only low- $Q$  region. The two approaches also yielded very close values for  $I_c(0)$ , 0.045 and 0.048 cm<sup>-1</sup> Å<sup>-1</sup>, respectively.

Using equation (4) and the protein concentration in the sample (determined by spectrophotometry) of 5.0 mg ml<sup>-1</sup> we estimate the linear density of the filament to be one monomer per 11.7 Å, or 5.4 monomers per turn. This should be considered as a very rough estimate, considering the uncertainty of the excluded volume and the scattering density of this particular protein. We also cannot exclude presence of some fraction of the protein in the monomeric form, which would contribute very little to the scattering intensity and lead to underestimation of the linear density of the filament. The value of one monomer per 11.7 Å, however, is reasonably close to that obtained for the crystal structure ( $\sim 11.2 \text{ \AA}$ ).

The helical pitch differed from the crystal structure (67 Å), and attempt to use the crystal geometry for the RecA helical filament resulted in a poorer fit of the data ( $\chi^2 = 3.1$  versus 1.2, figure 1(C)). Similar difference between the protein geometry in solution as compared to the crystal structure was observed, e.g., in *E. coli* RecA protein [7, 11]. Considering that RecA protein filaments are flexible structures that may

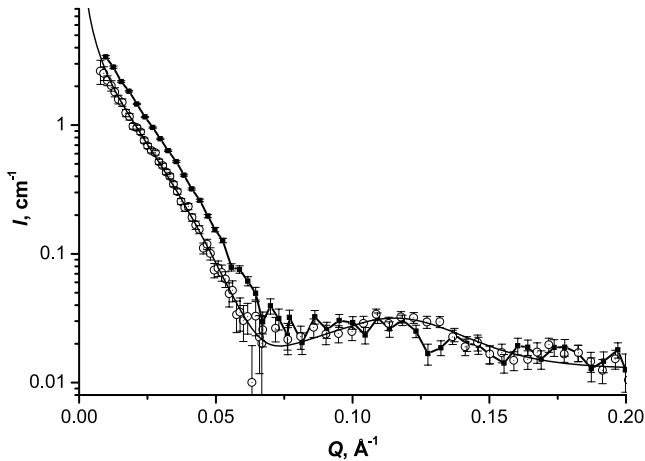


**Figure 2.** Scattering of the complex of RecA<sub>Dr</sub> with M13 ssDNA in the presence of ADP in D<sub>2</sub>O buffer containing 2 mM (squares) and 10 mM (circles) Mg<sup>2+</sup>. Data acquired on YuMO spectrometer.

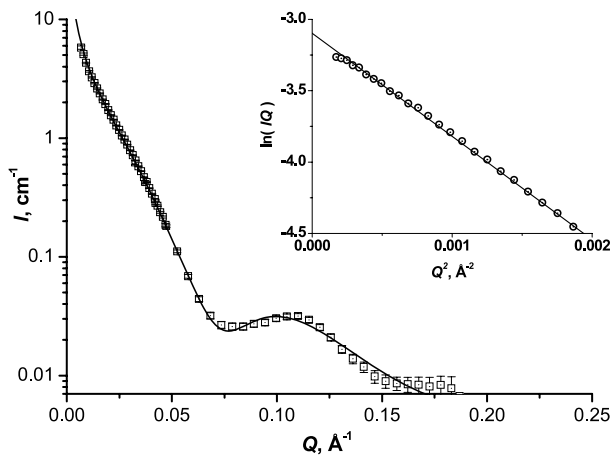


**Figure 3.** Scattering spectra of the complex of RecA<sub>Dr</sub> with ADP (2.5 mM) in D<sub>2</sub>O buffer acquired on D11 spectrometer. Inset shows Guinier plot for the low scattering angle region of the data in rod-like particle approximation. Data fitted to the model for long helical filament yielding helical pitch 67 Å and  $R_c = 40.7$  Å and  $I_c(0) = 0.043 \text{ cm}^{-1} \text{ Å}^{-1}$ .

undergo various conformational transitions depending on co-factor binding and solution properties (such as pH and ionic strength), it appears likely that the crystal structure reflects a somewhat stretched state of the protein as compared to the conformation assumed by the protein self-polymer in solution. Compared to RecA protein from *E. coli*, the structure of the filament in solution is significantly more compressed, exhibiting lower helical pitch (69 Å in *E. coli* protein).

Formation of the helical filament of RecA<sub>Dr</sub> complex with DNA required higher Mg<sup>2+</sup> concentration than in the case of *E. coli* enzyme. At 2 mM Mg<sup>2+</sup>, sufficient for formation of *E. coli* RecA filament, RecA<sub>Dr</sub> did not bind to ssDNA in the presence of ADP, but SANS spectra of such a complex lacked the subsidiary maximum indicative of a helical structure (figure 2). These data could not be described as a mixture of the active and inactive filaments and imply either a non-helical filament, or a system of helical filaments of varying geometry. This state

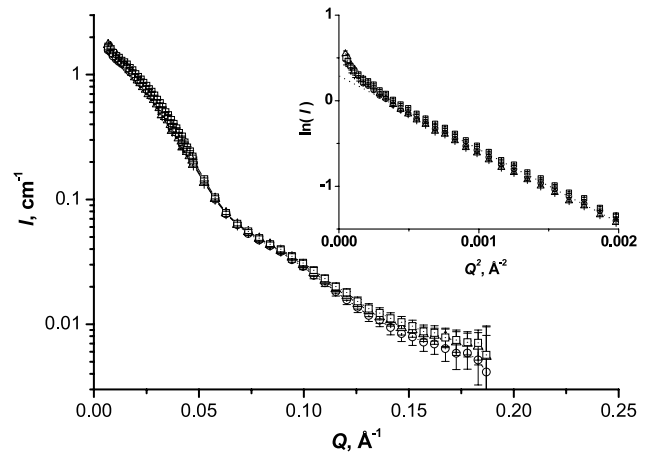


**Figure 4.** Scattering spectra of the complex of RecA<sub>Dr</sub> with ADP (2.5 mM) in D<sub>2</sub>O buffer containing NaCl in concentrations 0.6 M (squares), 1.2 M (circles) and 1.8 M (triangles). Inset shows Guinier plot for the low scattering angle region of the data with the linear fit corresponding to  $R_g = 50$  Å.

**Table 1.** Filament geometry for complexes of RecA protein from *D. radiodurans* with different co-factors.

Co-factors	Pitch (Å)	$R_c$ (Å)	Monomers per turn
<i>Inactive filament</i>			
Mg <sup>2+</sup>	63	39.8	5.4
Mg <sup>2+</sup> , ADP	67	40	5.1
Mg <sup>2+</sup> , ADP, ssDNA	69	40.1	5.2
<i>Active filament</i>			
Mg <sup>2+</sup> , ATPγS, HSC	87	36.8	5.3
Mg <sup>2+</sup> , ATPγS, ssDNA	88	36.1	5.3
Mg <sup>2+</sup> , ATPγS, dsDNA	88	36.9	5.5

of RecA protein may be similar to the disordered filaments, which were observed for Rad51 proteins [18, 19], but not for bacterial RecA. At 10 mM Mg<sup>2+</sup> the scattering spectrum of the complex RecA<sub>Dr</sub> with ssDNA and ADP shows a clear subsidiary maximum.

We have also observed much lower stability of RecA<sub>Dr</sub> filament formed in the presence of ADP toward increased ionic strength of the solution. In the absence of NaCl the scattering data were consistent with inactive helical filament (figure 3) with the pitch of 67 Å, cross-sectional gyration radius of 40 Å and the filament density estimated at one monomer per 13 Å (table 1). At NaCl concentrations of 0.6 M and higher (high salt conditions, HSC), SANS spectra were inconsistent with this model (figure 4). Instead, under these conditions the scattering intensity at small  $Q$  (figure 4, inset) followed Guinier law, allowing to estimate the gyration radius of the species at  $\sim 50$  Å and their mass (calculated using equation (3)) at 7.5 monomers. There was, however, some increase in the scattering intensity at the very small angles, pointing to the presence of larger protein aggregates. We found that these data can be reasonably well described by a mixture of oligomers with  $R_g \sim 50$  Å and rod-like polymers seen in the absence of NaCl with  $R_c = 40$  Å



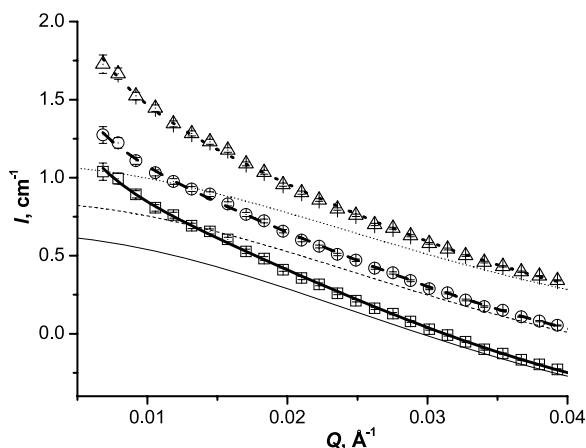


**Figure 5.** Low- $Q$  region of the spectra shown in figure 4 (data for 0.6 and 1.2 M NaCl are offset for clarity by  $-0.6$  and  $-0.3$   $\text{cm}^{-1}$ , respectively). Each data set was fitted to the linear combination of Gaussian term (shown in thin lines) and a Guinier approximation for scattering by rod-like particles with  $R_c$  of  $40$   $\text{\AA}$  (overall fits shown in heavy lines). Approximated zero-angle intensities for the two terms were used to evaluate the size and mass fraction of protein oligomers (see the text).

(figure 5). The ratio of the two protein forms was estimated as

$$\frac{C_{\text{ring}}}{C_{\text{filament}}} = \pi \frac{I_r(0)}{I_c(0)} \frac{\mu}{M_r},$$

where  $I_r(0)$  and  $I_c(0)$ —approximated intensities at zero angle for the ring and the filament components of scattering obtained from the fit in Figure 5,  $\mu$  is the mass per unit length of the filament and  $M_r$  is the molecular weight of the oligomer. Based on the data shown in figure 5 we estimate that at HSC between 88 to 94% of the protein existed in the form of oligomers. The estimate for the mass of the oligomers was between 6.9 and 7.6 monomer mass and the gyration radius was between 49.5 and 50.1  $\text{\AA}$ .

Our estimate for the mass of the oligomer contains the same uncertainties as the estimate for the linear density of the filament, mentioned above. Additionally, the observed deviation from the linearity in Guinier region of the curve may be caused by the presence of an aggregated form of the protein other than filaments. Indeed, apparent decrease in the fraction of the oligomeric form in favor of the larger polymer as the salt concentration increases seems to suggest that the filaments seen in the absence of NaCl differ from the large particles seen under HSC. However, as we have seen above, taking into account the contribution to scattering by these aggregates did not affect dramatically our estimate for the oligomer mass and particularly its radius of gyration. Thus, under HSC the predominant species of RecA<sub>Dr</sub> appear to be small oligomers, presumably ring-like structures observed for other homologous recombinases. Molecular modeling of the ring structures of RecA<sub>Dr</sub> seems to suggest that hexameric ring is in a better agreement with the  $R_g$  value of 50  $\text{\AA}$  than the heptamer or octamer (data not shown).

On the other hand, we found that protein complex with ATP $\gamma$ S forms stable filaments under HSC. In a buffer containing 1.8 M NaCl and 2.5 mM ATP $\gamma$ S the pitch of

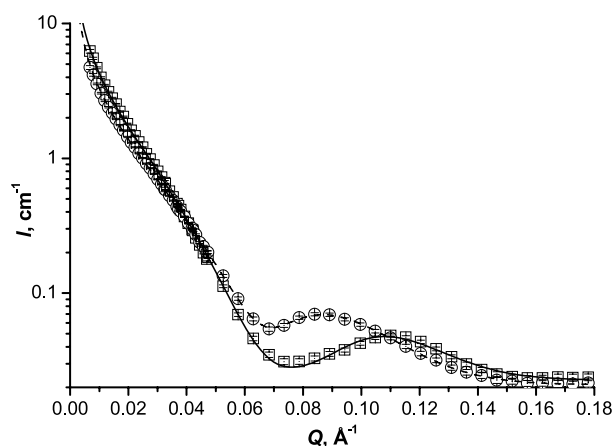


**Figure 6.** Stretching of RecA<sub>Dr</sub> filament in D<sub>2</sub>O buffer containing 1.8 M NaCl and 2.5 mM ATP $\gamma$ S. Best-fit parameters for the helical pitch and cross-sectional gyration radius are 87 and 36.7  $\text{\AA}$ , respectively.

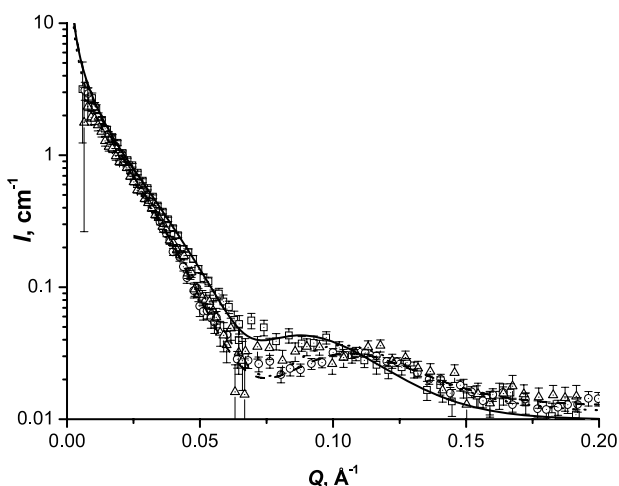


**Figure 7.** Scattering of the complexes of RecA<sub>Dr</sub> protein with ssDNA in D<sub>2</sub>O buffer containing 10 mM Mg<sup>2+</sup>. Data acquired on YuMO spectrometer and fitted to the model for long helical filament. Squares: 2.5 mM ATP $\gamma$ S,  $R_c = 37$   $\text{\AA}$ , pitch 85  $\text{\AA}$ ; triangles: 2.5 mM ADP and 1 mM Al(NO<sub>3</sub>)<sub>3</sub>/5 mM NaF,  $R_c = 40$   $\text{\AA}$ , pitch 63  $\text{\AA}$ ; circles: 0.5 mM ATP $\gamma$ S,  $R_c = 38$   $\text{\AA}$ , pitch 70  $\text{\AA}$ .

the filament was 87  $\text{\AA}$ , the cross-sectional radius of gyration  $\sim 36.8$   $\text{\AA}$  and the estimated density of one monomer per 16.4  $\text{\AA}$  (figure 6). Thus, ATP $\gamma$ S appears to have stabilizing effect on the filament, while ADP seems to decrease its stability. Filaments of RecA<sub>Dr</sub> formed in complex with ATP have been reported to have higher stability in HSC than *E. coli* RecA [20]. We also see that similar to *E. coli* protein, HSC appear to induce transition of RecA<sub>Dr</sub> to the active conformation (table 1).

Formation of the presynaptic complex of the enzyme required higher concentration of ATP $\gamma$ S (2.5 mM, compared to  $<0.5$  mM for *E. coli* RecA) and transition from the inactive to the active form of the filament in the presence of an ADP–AlF<sub>4</sub> complex, which is another widely used ATP analog, did not occur (figure 7). Lower affinity of this enzyme toward ATP and

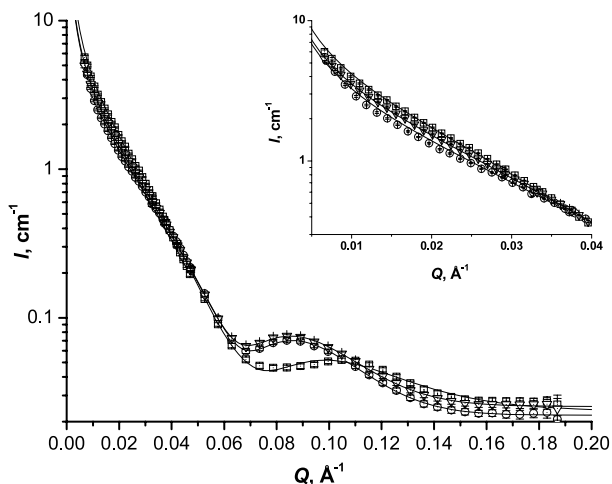


**Figure 8.** Scattering of the complexes of RecADr protein with ssDNA and dsDNA in a D<sub>2</sub>O buffer. Inset shows the region of low Q of the data. Data fitted to the model for long helical filament. Squares: protein complex with ssDNA and ADP, pitch 69 Å,  $R_c = 40.1$  Å,  $I_c(0) = 0.042$  cm<sup>-1</sup> Å<sup>-1</sup>; circles: ssDNA and ATPγS, pitch 88 Å,  $R_c = 36.9$  Å,  $I_c(0) = 0.034$  cm<sup>-1</sup> Å<sup>-1</sup>; triangles: dsDNA and ATPγS, pitch 89 Å,  $R_c = 36.1$  Å,  $I_c(0) = 0.034$  cm<sup>-1</sup> Å<sup>-1</sup>.

ADP could be implicated from ATP hydrolysis data reported earlier [2]. Formation of the active complex of the enzyme with ssDNA resulted in a significant stretching of the protein filament (figure 8). This complex of the protein with ssDNA was characterized by an increased helical pitch (to 88 Å) as well as decreased cross-sectional gyration radius (to ~36.1 Å). Similar conformational state was observed for the filaments of several other RecA proteins [7, 11].

Despite significant stretching of the filament, the number of monomers per helix turn (5.3, or one monomer per 16.5 Å) did not appear to change when compared to the inactive protein polymer. Inactive complex of RecA<sub>Dr</sub> with ssDNA formed in the presence of ADP (pitch 69 Å,  $R_c = 40.1$  Å) also has similar density (one monomer per 13.3 Å, 5.2 monomers per turn). One could expect that any significant change in the number of monomers per turn during conformational transition would require extensive unwinding or disassembly of the filament. Although in the earlier works the transition between active and inactive filament of *E. coli* RecA has been reported to involve change in the filament mass per turn [7], the later models suggest the number of monomers per turn to be very similar in different conformations of the filaments [9, 21, 22].

One of the unusual features of RecA protein from *D. radiodurans* is its affinity to dsDNA. Unlike other RecA proteins that preferentially bind to ssDNA, in competition experiments where both ssDNA and dsDNA, this protein formed presynaptic complex with dsDNA, followed by homologous binding and strand exchange with ssDNA [3]. SANS data obtained for the complex of this protein with dsDNA show that its geometry is almost identical to the geometry of the similar complex with ssDNA (figure 8). The helical pitch of the filament was 88 Å and the gyration radius around 36.9 Å (5.5 monomers per turn). Similar results were obtained for *E. coli* enzyme [8, 13, 21], in particular, in

work [21] very little structure difference was found between filaments formed on ssDNA and dsDNA.

Our data indicate that despite the difference in function and the monomer structure, on the large scale the behavior of RecA<sub>Dr</sub> is very similar to RecA from *E. coli*, although compared to the latter enzyme, filaments of RecA<sub>Dr</sub> exhibited lower stability in high salt and lower affinity toward co-factors such as Mg<sup>2+</sup> and ATP analogs. Filaments of RecA protein from *D. radiodurans* can assume ‘open’ and ‘closed’ conformation, similar to those seen in RecA proteins from *E. coli* and *P. aeruginosa* [7–10]. Large N-terminal domain of RecA<sub>Dr</sub> does not seem to hinder this motion, which in case of *E. coli* RecA filament can be explained by a coordinated rotation of two neighbouring amino acids forming a single hinge in the N-terminal domain of the protein [22]. The data also show that just like ssDNA, dsDNA binding results in stretching of the enzyme in the active form, with the pitch increasing to the value conservative for a number of RecA proteins and their functional analogs.

## Acknowledgments

This work was supported by the Russian Foundation for Basic Research (grants No. 02-04-49259-a and No. 07-04-01548-a), Russian Academy of Science programs ‘Physics of Elementary Particles’ (subprogram ‘Neutron physics’, direction ‘Studies of structure, dynamics and non-ordinary properties of matter by neutron scattering’) and Ministry of Science and Education program RNP 2.2.1.1.4663. The authors are very grateful to Dr Mikhail Petukhov and Dr Michael M Cox for their help and useful discussions.

## References

- [1] Battista J R 1997 *Annu. Rev. Microbiol.* **51** 203–24
- [2] Kim J-I, Sharma A K, Abbott S N, Wood E A, Dwyer D W, Jambura A, Minton K W, Inman R B, Daly M J and Cox M M 2002 *J. Bacteriol.* **184** 1649–60
- [3] Kim J-I and Cox M M 2002 *Proc. Natl Acad. Sci. USA* **99** 7917–21
- [4] Rajan R and Bell C E 2004 *J. Mol. Biol.* **344** 951–63
- [5] Story R M, Weber I T and Steitz T A 1992 *Nature* **355** 318–25
- [6] Xing X and Bell C E 2004 *J. Mol. Biol.* **342** 1471–85
- [7] DiCapua E, Schnarr M, Ruigrok R W, Lindner P and Timmins P A 1990 *J. Mol. Biol.* **214** 557–70
- [8] Ellouze C, Takahashi M, Wittung P, Mortensen K, Schnarr M and Norden B 1995 *Eur. J. Biochem.* **233** 579–83
- [9] Yu X, Jacobs S A, West S C, Ogawa T and Egelman E H 2001 *Proc. Natl Acad. Sci. USA* **17** 8419–24
- [10] Lebedev D V, Baitin D M, Islamov A, Kuklin A I, Shalguev V, Lanzov V A and Isaev-Ivanov V V 2003 *FEBS Lett.* **537** 182–6
- [11] Bell C E 2005 *Mol. Microbiol.* **58** 358–66
- [12] Xiao J and Singleton S F 2002 *J. Mol. Biol.* **320** 529–58
- [13] Sattin B D and Goh M C 2004 *Biophys. J.* **87** 3430–6
- [14] Shibata T, Cunningham R P and Radding C M 1981 *J. Biol. Chem.* **256** 7557–64
- [15] Ostanevich Y M 1988 *Macromol. Symp.; J. Makromol. Chem.* **15** 91–103
- [16] Zakharova S S, Jesse W, Backendorf C, Egelhaaf S U, Lapp A and van der Maarel J R C 2002 *Biophys. J.* **83** 1106–18
- [17] Svergun D I and Fejgin L A 1986 *Rentgenovskoe i Neitronnoe Malouglovoe Rasseyanie* (Moscow: Nauka) pp 66–75

- [18] Ellouze C, Kim H-K, Maeshima K, Tuite E, Morimatsu K, Horii T, Mortensen K, Norden B and Takahashi M 1997 *Biochemistry* **36** 13524–9
- [19] Ristic D, Modesti M, van der Heijden T, van Noort J, Dekker C, Kanaar R and Wyman C 2005 *Nucleic Acids Res.* **33** 3392–402
- [20] Kim J-I 2006 *J. Microbiol.* **44** 508–14
- [21] Frykholm K, Morimatsu K and Norden B 2006 *Biochemistry* **45** 11172–8
- [22] Petukhov M, Lebedev D, Shalguev V, Islamov A, Kuklin A, Lanzov V and Isaev-Ivanov V 2006 *Proteins* **65** 296–304